

Analysis and Performance Investigations on a Solar Air Heater with Compound Parabolic Concentrator

D.K.Patel*

Mechanical Engineering Department, Government
Engineering College ,Patan
Research Scholar , Rai University, Ahmadabad
India

e-mail: dkpatel09@gmail.com

P. K.Brahmbhatt

mechanical engineering department, government engineering
College ,Modasa
Research Guide , Rai University, Ahmadabad
India

e-mail:pragneshbrahmbhatt@gmail.com

Abstract— The numerical simulation for computing the thermal performance of an air heater with a truncated compound parabolic concentrator (CPC) having a flat one-sided absorber and experimental validation of a compound parabolic concentrator (CPC) are presented. The solar device had an aperture area of 1.2m^2 , a real concentration ratio of 2, an acceptance half angle of 30° , and an aluminium flat receiver coated with a commercial selective surface. The profile of an air heater with a truncated is generated through programming with Auto LISP developed for construction of Compound parabolic concentrator (CPC) having a flat one-sided absorber which does not require any tilt adjustment. The effect of the air mass flow rate, the wind speed and the collector length on the thermal performance of the air heater is investigated by computer code that employs an iterative solution. A low cost solar air heater with CPC was fabricated and experimentally tested at Patan, North Gujarat (23.4°N , 72°E) and operating performances is to be determined Experimental tests were performed using air as working fluid and the mass flow rates from 0.012 kg/s and 0.016 kg/s . A comparison of the experimental results with the numerical model developed was carried out. The results of the thermal efficiency, outlet temperature, were compared and found to be in close agreement with the experimental data. Therefore, the model is a reliable tool for the design and optimization of solar air heater with compound parabolic concentrator.

Keywords- solar concentrators, reflectors, solar air heater, compound parabolic concentrator, Autolisp

I. INTRODUCTION

Compound parabolic concentrator (CPC) is a non-imaging type concentrating solar collector where the incident rays, after reflection from the reflector, are not focused at a point or line but are simply collected on absorber (receiver) surface. The concentration ratio C , which is defined as the ratio of aperture area to absorber area is generally 2 to 10. CPC achieves the ideal concentration ($C=1/\sin\theta_c$). It is generally oriented in E-W direction. It does not need a continuous tracking of the sun but it necessitates only a few tilt adjustments per year. The rays incident in the range of acceptance angle $2\theta_a$ are fully accepted by CPC..

The name, CPC, derives from the fact that it consists of two parabolic mirror segments with different focal points. The angle between the axis of the CPC and the line connecting the focus of one of the parabolas with the opposite edge of the aperture is the acceptance half angle θ_a . CPCs consist basically of three elements Receiver The receiver should have the highest absorptance for solar radiation as possible and must be constructed with high-conductivity metals in order to conduct efficiently the absorbed heat into the heat transfer fluid. Most receiver materials do not have a very high absorptance, and they need to be covered with special solar selective surface coatings [1]. A commercial selective surface for applications in solar energy made from a silicon polymer, with an emissivity from 0.28 to 0.49 and absorptance values from 0.88 to 0.94 was applied on the surface of this receiver. Cover The ideal cover is a transparent insulation that allows the passage of solar radiation to the reflector and receiver, having a high transmittance of solar radiation, and a low transmittance of the thermal radiation from the receiver; also, it must have high durability and low cost. The cover used was a low-iron tempered glass with a thickness of 4 mm. Reflector Reflectors

for solar concentrators should have the highest reflectance as possible. Its function is to focus beam-solar radiation onto the receiver, which is located at the focus of the system. Two aluminum sheet segments with a reflectance of 0.87 were used to construct the reflector sides.

II. LITERATURE REVIEW

Yan et al. [2] developed a dynamic model of solar parabolic trough collectors applied as direct steam generation systems. The model was solved by an explicit Euler's method and considered different working conditions and thermal parameters. The simulated results were validated using two real test data on typical summer and winter days, and the steam -generating process from unsaturated water to superheated steam was studied. The relationship between output steam features and solar radiation, inlet water temperature, mass flow rate, and collector area were evaluated.

Odeh and Morrison [3] developed a transient simulation model to analyze the performance of industrial water heating systems by using parabolic trough solar collectors. The system consisted of a parabolic trough collector with a glass cover, a back-up boiler, and a thermal storage tank. The high-accuracy model was applied to optimize the system operation during transient radiation periods. Kim et al. [4] researched the thermal performance of evacuated CPC solar collector with a cylindrical receiver and analyzed a numerical model based on the irradiation determined in each moment; they concluded that the numerical model could accurately estimate the performance of the solar collectors. Tchinda and Ngos [5] developed mathematical equations to study the thermal processes in a CPC collector with a flat one-side receiver with various dimensions. The results showed that for a given length, the efficiency increased as the flow rate increased, and the outlet temperature of the heat transfer fluid decreased with an

increase of mass flow rate; the selective coating and the nature of the reflector material changed considerably the thermal performance of the CPC. Pramuang and Exell [6] developed a method to determine the performance parameters (the optical efficiency, the heat loss coefficients, and the effective heat capacity) of a truncated CPC applied to an air heater under non-steady conditions. The optical efficiency and the first order loss coefficient agreement were around 2% and 3%, respectively. They concluded that their method could be applied at any time of the year in variable tropical climates where a steady state method was not possible. Prapas et al. [7] investigated the flow distributions through the receiver tubes of a CPC collector for both east–west (E–W) and north–south (N–S) alignments of the system. The results showed that the flow distribution was non-uniform in an E–W alignment, compared with a close approximation to a uniform distribution for the N–S alignment. However, both alignments presented a similar thermal state performance of the concentrator. Fraidenraich et al. [8] developed a mathematical model for the optical and thermal performance of non-evacuated CPC solar collectors with a cylindrical receiver, where the heat loss coefficient was temperature dependent. The numerical results presented the performance of the solar collector by a set of curves, one for each radiation level. Prasad and Tiwari [9] developed a thermal analysis of a concentrator-assisted solar distillation unit to optimize the glass cover inclination. The solar device was a CPC. An analytical expression for the air mass flow rate, wind speed and the collector length on the thermal performance of the air heater ,an instantaneous thermal efficiency was carried .

III. RESEARCH METHODOLOGY

Winston, R., Minaco, J.C., Benitez, P., Shatz, N., & Bortz, J.C.(2005) used a mathematical description of the CPC in polar coordinates according to Eqs. 1~5 for construction of a two dimensional CPC. It is simplest to obtain the basic properties of the CPC from the equation of the parabola in polar coordinates for developing AutoLISP program for generating profile of CPC [10].

$$R = \frac{2f_l}{1 - \cos(\phi)} \quad (1)$$

$$r = R \sin(\phi - \theta_{\max}) - a' = \frac{2f_l \sin(\phi - \theta_{\max})}{1 - \cos \phi} - a' \quad (2)$$

$$z = R \cos(\phi - \theta_{\max}) = \frac{2f_l \cos(\phi - \theta_{\max})}{1 - \cos \phi} \quad (3)$$

$$f = a'(1 - \cos(90 + \theta_{\max})) = a'(1 + \sin \theta_{\max}) \quad (4)$$

f_1 is the focal length of the parabolas.

$$2a' = \frac{2f_l}{1 - \cos(90 + \theta_{\max})} \quad (5)$$

IV GEOMETRICAL CONSTRUCTION OF CPC PROFILE

Auto LISP is a powerful programming language that quickly create own commands, routines. It is a programming language that can greatly enhance productivity by automating often-used or repetitive tasks. This feature-rich software is used in AutoCAD® to specify points, do calculations and speed up repetitive tasks using macros. For using Auto LISP program in AutoCAD®, Auto LISP file can be load from within Visual LISP or from within AutoCAD®. AutoCAD® offers lsp files which can be used for Auto LISP routings as acad.lsp. Auto LISP program is developed for geometrical profile generation of CPC from polar coordinate equations and file save as cpc.lsp. “Fig.1” shows the generated Profile of CPC by adding two variables half acceptance angle θ_a and aperture length L_2 in loaded cpc.lsp file of AutoCAD® [11-12].

Some Operation for CPC Autolisp Program

```
(defun c:cpc ()
  (setq l2 (getreal"\n enter the length-"))
  (setq th (getreal"enter the angle-"))
  (setq thR (/ (* th pi) 180))
  (setq sine (sin thR))
  (setq cose (cos thR))
  (setq tan (/ sine cose))
  (setq pr1 (list x2 y1))
  (command "pline" pl1 pr1 "")
  (setq fl (/ (+ 1 sine) l1) 2))
  (setq x (- (/ (* 2 fl (sin (- fy thr))) (- 1 (cos fy))) (/ l1
  2)))
  (setq pl1 (list(car pl2) (cadr pl2)))
  (setq pr1 (list(car pr2) (cadr pr2)))
  (setq y (+ y 0.1))
```

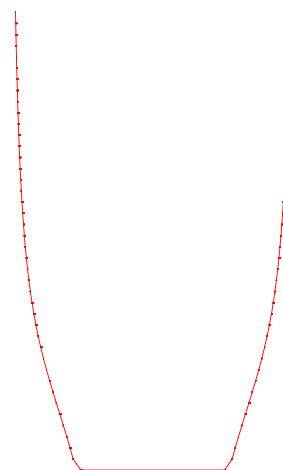


Figure 1. Geometric Profile of CPC ($\theta_a = 30^\circ$, $L_2 = 100$)

V RAY TRACE OF CPC

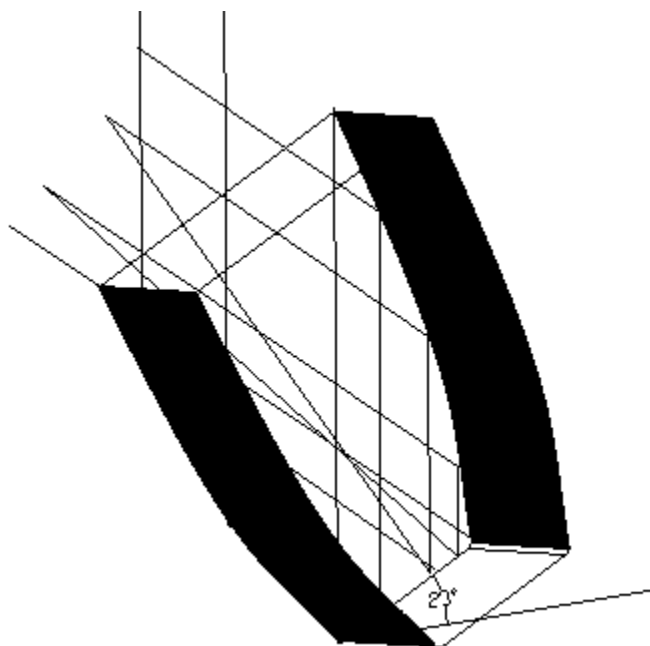


Figure 2.: CPC ray trace at latitude angle ($\theta_a = 30^\circ$, $L2=100$).

In order to investigate the location of the hot spots on the absorber, a ray trace is needed. The objective is threefold. Firstly it is necessary to calculate the profile of the CPC. Secondly, it is necessary to analyze the distribution of intensity around the absorber, finally, to analyze the phenomena of the rays inside the CPC for different incident angle. AutoCAD® allows mathematics and graphics to be combined to produce ray traces of various complexities which are visually accurate. To deal with first part of the problem, Auto LISP programming is used to calculate (x, y) Co-ordinate of the profile of the CPC and the absorber and a drawing of the profile of the CPC reflector and absorber is produced. This is then scaled up to show the precise points where the rays are expected to hit the reflector. A normal is drawn from these points. The rays is mirrored from the normal with the same angles and extended and repeated until they reached the absorber. The Fig. 2 shows CPC ray trace and profile generated through Auto LISP and tilted at a latitude angle (23°) with length 30mm [13-14].

VI ANALYSIS

Applying heat balancing in suitable way, the following partial differential equations can be derived

For the transparent cover

$$M_c C_{cp} \frac{\partial T_c}{\partial t} = q_c(t) + h_{rp}(T_p - T_c) + h_{p/c}(T_p - T_c) - h_{rs}(T_c - T_s) - h_{c/a}(T_c - T_b) \quad (6)$$

For the flat absorber

$$M_p C_{pp} \frac{\partial T_p}{\partial t} = q_p(t) - h_{rp}(T_p - T_c) - h_{p/c}(T_p - T_c) - q_u(t) \quad (7)$$

For the fluid

$$p_r e_r C_{pf} \frac{\partial T_f}{\partial t} = q_u(t) - \frac{\dot{m} C_{pf} \partial T_f}{l_p \partial x} - U_o(T_f - T_b) \quad (8)$$

With $t > 0$ and $0 < X < L$.

In Eqs. (6) and (7), $q_c(t)$ and $q_p(t)$ have been expressed using Hsieh's theory, as

$$q_c(t) = I(t) [\bar{\alpha}_c + \bar{\alpha}_c \bar{\tau}_c \bar{\rho}_p \rho_m^{2(n)}] \frac{A_c}{A_p} \quad (9)$$

$$q_p(t) = I(t) \bar{\tau}_c \rho_m^{(n)} P [\bar{\alpha}_p + \bar{\alpha}_p \bar{\rho}_p \bar{\rho}_c \frac{A_p}{A_c}] \frac{A_c}{A_p} \quad (10)$$

P is the gap loss factor, which is equal to $1-g/l_p$, where g is the gap thickness. $A_c = W*L$ and $A_p = l_p*L$

At any point x, the fluid temperature (T_f) is related to the useful energy q_u (see Eqs. (7) and (8)) and the absorber temperature (T_p) by the following expression

$$q_u = U_f(T_p - T_f) \quad (11)$$

The factor U_f is the convective heat transfer coefficient between the heat transfer fluid and the walls of the absorber. It is calculated from the relationship

$$U_f = \frac{N_{uf} \lambda_f}{D_H} \quad (12)$$

Where the Nusselt number N_u and the hydraulic diameter D_H

Assuming that the overall heat loss coefficient U_L and the collector efficiency factor are temperature independent in position, the efficiency is found to be

$$\eta_{inst} = \frac{Q_u}{A_c I(t)} \quad (13)$$

Where the useful thermal power Q_U extracted from the CPC collector is calculated from the relationship

$$Q_u = F_R A_T [S_p - U_L (T_{fe}(0, t) - T_b(t))] \quad (14)$$

F_R is a removal factor given by:

$$F_R = \frac{C_{pf} \dot{m}}{l_p L U_L} \left(1 - e^{\left(\frac{-l_p L F' U_L}{C_{pf} \dot{m}} \right)} \right) \quad (15)$$

Using Eqs. (14) And (15) η_{inst} becomes

$$\eta_{inst} = (\eta_o + F_A) F_R - \frac{U_L}{C_a I(t)} F_R (T_{fc}(0, t) - T_b(t)) \quad (16)$$

Where the optical efficiency is given by:

$$\eta_o = \bar{\tau}_c \rho_m^{(n)} \bar{\alpha}_p P \left(1 + \bar{\rho}_p \rho_c \frac{l_p}{2W} \right) \quad (17)$$

The heat loss coefficient by convection $h_{c/a}$ between the cover and the ambient is correlated by Duffie and Beckman as the optical efficiency is given by :

$$\eta_{o1} = \bar{\tau}_c \rho_m^{(n)} \bar{\alpha}_p \quad (18)$$

Parameter	Symbol	Value
Acceptance half angle	θ_a	30°
Cover absorptance	$\bar{\alpha}_c$	0.2
Flat plate absorber absorptance	$\bar{\alpha}_p$	0.95
Cover transmittance	$\bar{\tau}_c$	0.89
Cover emittance	ϵ_c	0.85
Flat plate absorber emittance	ϵ_p	0.91
Cover reflectance	ρ_c	0.05
Reflector reflectance	ρ_m	0.86
Flat plate absorber reflectance	$\bar{\rho}_m$	0.15

TABLE I.THE CHARACTERISTICS OF THE CPC'S

VII. NUMERICAL INPUTS

Meteorological data

To have a numerical appreciation of the developed analysis, calculations have been performed corresponding to the mean values of the ambient temperature and global radiation in May at Patan, North Gujarat (23.4°N, 72°E).

Heat-transfer coefficients

The different heat transfer coefficients for each surface in the present systems are evaluated as follows.

Radiation heat transfer from the cover to the sky,

The radiative h_{Rp} heat transfer coefficient between the flat plate absorber and the cover is

$$h_{Rp} = \frac{\sigma(T_p^2 + T_c^2)(T_p + T_c)}{\frac{1}{\epsilon_p} + \frac{A_p}{A_c} \left(\frac{1}{\epsilon_c} - 1\right)} \tag{19}$$

Radiation heat transfer from the flat plate absorber to the cover

The radiative heat loss coefficient h_{Rs} between the cover and the sky is calculated from the relationship

$$h_{Rs} = \sigma\epsilon_c(T_p^2 + T_c^2)(T_p + T_c) \frac{A_c}{A_p} \tag{20}$$

Where the expression of the sky temperature is give by Hsieh

$$T_s = T_b - 6 \tag{21}$$

Convection heat transfer coefficient from the cover due to wind,, The heat loss coefficient by convection $h_{c/a}$ between the cover and the ambient is correlated by Duffie and Beckman as:

$$h_{c/a} = (5.7 + 3.8v) \frac{A_c}{A_p} \tag{22}$$

[15]According to the Hsieh theory the convective $h_{p/c}$ heat transfer between absorber and the cover is

$$h_{p/c} = \left(3.25 + 0.0085 \frac{T_p - T_c}{2D_H}\right) \frac{A_c}{A_p} \tag{23}$$

Where

$$D_H = \frac{2l_p e_r}{l_p + e_r} \tag{24}$$

The flow is assumed to be hydro dynamically full developed at the collector inlet. The inner surface convective heat transfer coefficients were modeled according to the flow regime.

For laminar flow ($Re < 2100$) by the Mercer correlation

$$N_u = 4.9 + \frac{0.0606((R_e P_r D_H)/L)^2}{1 + 0.0909((R_e P_r D_H)/L)^{0.7} P_r^{0.17}} \tag{25}$$

For turbulent flow ($Re > 2100$) by the Kays correlation presented in a mathematical form by Duffie and Beckman[16].

$$N_u = 0.0158 R_e^{0.8} \tag{26}$$

With

$$R_e = \frac{\dot{m} D_H}{l_p e_f \mu_f}, \quad P_r = \frac{\mu_f C_f}{\lambda_f}$$

The effects of wind on the instantaneous efficiencies are shown in fig.3. By decreasing the value of the wind speed ,as expected , the wind heat transfer coefficient decreases, and thus the overall loss coefficient value.

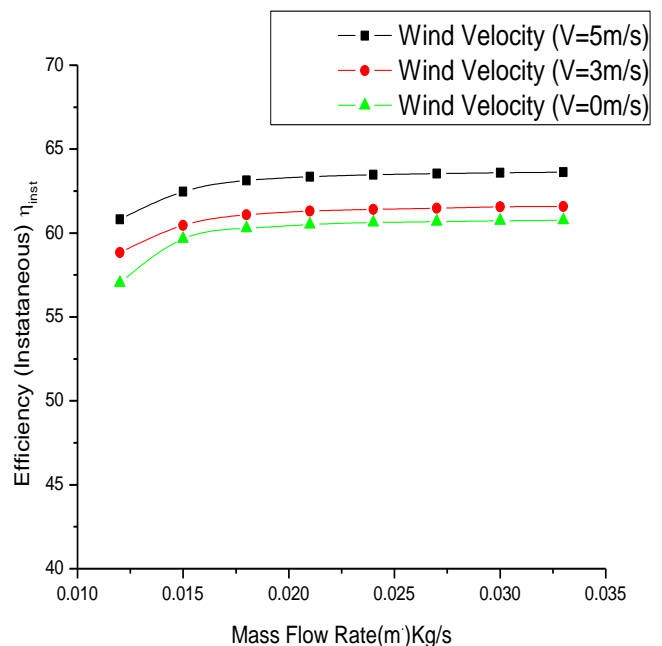


Figure 3. Effect of the air mass flow rate on the efficiency for three values of wind speed

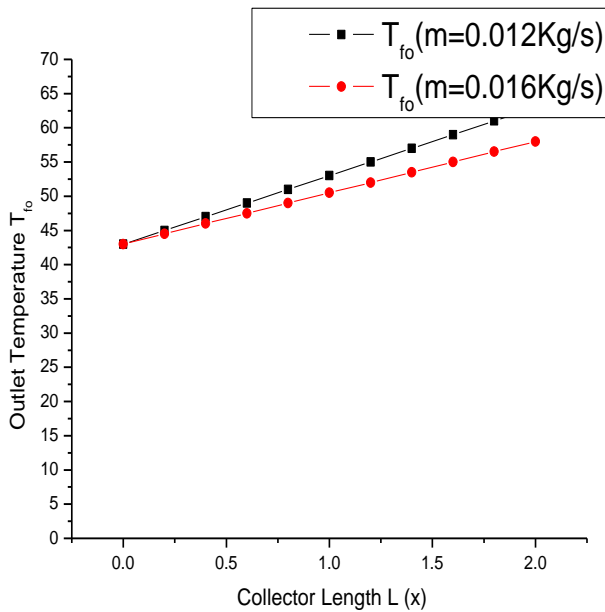


Figure 4. The outlet temperature at time 12.30pm as a function of the collector length for some values of the air mass flow rate

The effect of increasing collector length on the thermal performance is displayed in fig.4 and 5. As collector length is increased the absorber average temperature hence outlet temperature is appreciably increased. However instantaneous efficiencies slightly decrease with the increase in length of the collector which presumably results from the greater heat losses to the surroundings.

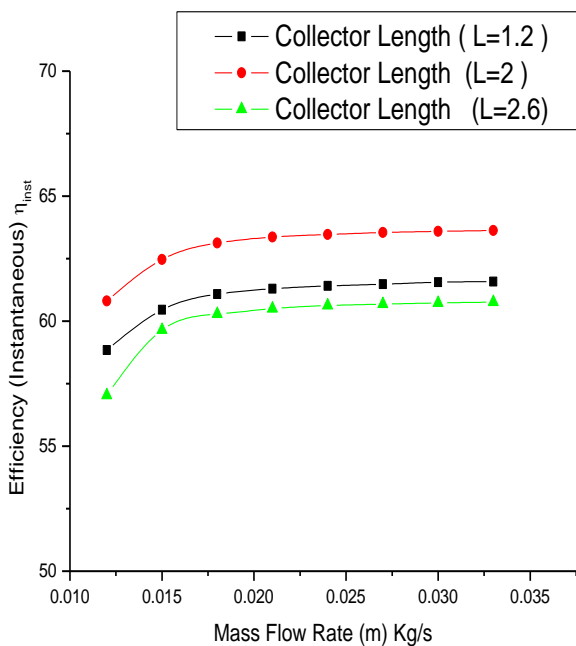


Figure 5. Effect of the air mass flow rate on the efficiency of the collector for the three value of L at time 12.30p.m.

VIII. FABRICATION METHODOLOGY

D.K.Patel and P.K.Brahmbhatt [17] designed and manufactured Compound parabolic solar air collector. The factors which affect the performance of a solar collector include (i) the environmental factors (ambient temperature, solar radiation characteristics, latitude, altitude of location, wind speed.etc.) and (ii) the design variables (dimensions, material and thermal characteristics). The effect of the environmental factors are external and may not be easily altered for improved performance, thus only design variables are left as the only ones that may be considered for optimal collector performance. Auto LISP generated profile of CPC with acceptance half-angle 30° and aperture width 60cm for the full and truncated solar air collector was printed to scale as printing templates and used in the construction of the reflector support and profile. The printed ‘CPC profile generated by Auto LISP’ design templates was then glued to the wooden supporting plates, which was pre-cut with measuring dimensions of (30x60x80cm), for the full profile as shown in fig.1. The respective profiles were cut out using a saw and assembled in the laboratory. This technique gave an accurate profile and structure supports. and a rigid exo-skeleton framework supported the reflective panels of the collector. Anodized aluminium with a specular reflectance of approximately 80% is rolled as per Wooden templates profile for reflector. The collector assembly was placed in a location where there was access to sunlight and throughout the experiment, the collector was kept with its absorber aligned east-west with the tilt angle being the latitude of the place (23.4°) towards south so as to maximize useful solar energy. Air was used as the heat transfer fluid. One collector panel with CPC truncated of the full size within the acceptance half angle of 30° is fabricated. The collector has a total aperture area of 1.2 m² and a flat plat absorber area of 0.48m².



Figure 6. Picture to show the prototype of CPC Solar Air Collector.

This collector has overall dimensions of 0.8m height, 0.6m aperture width, 0.3m receiver width and 1.6m length the receiving surface which is black GI V-shaped corrugated absorber plate for improving the value of the heat transfer coefficient between the absorber plate and the air thus result in a higher efficiency forms the upper side of a rectangular airflow duct of depth 0.15m made of GI sheet 0.5 mm thick. The bottom of the duct is insulated with glass wool 50mm thick as shown in fig.6 [18-20]. Some of the factors to be considered in designing the parabolic structure were that it was not distort significantly due to its own weight and able to withstand wind loads.

IX. EXPERIMENTAL METHODOLOGY

The performance test of the prototype was carried out with glazing and thermal insulation including rectangular airflow duct, and total weather station at the Patan, North Gujarat (23.4°N, 72°E). In the experiment we measured the readings of global radiation H_t , absorber temperature T_r , reflector temperature T_m , cover temperature T_a , air inlet temperature T_i , air outlet temperature T_o and ambient temperature T_b , was taken for two mass flow rates m (0.012 kg/s and 0.016 kg/s) from 8 a.m. to 5p.m. at the interval of 1 hour in the month May. In this study The absorber was made of galvanized iron sheet with black chrome selective coating and thickness of plate was 0.5mm. The cover window type, the Plexiglass of 3mm thickness, was used as glazing. Thermocouples were positioned evenly, on the top surface of the absorber plates along the direction of flow at identical positions for measuring inlet and outlet air temperatures. The output from thermocouples was recorded in degrees Celsius by using a digital thermocouple thermometer ADI111 measurement range -50 to 1300 °C; resolution 1°C, accuracy, ±2.2°C. as digital thermometer measured the ambient temperature with sensor in display LCD placed in a special container behind the collectors' body. The total solar radiation incident on the surface of the collector was measured with a total weather station Pyranometer.

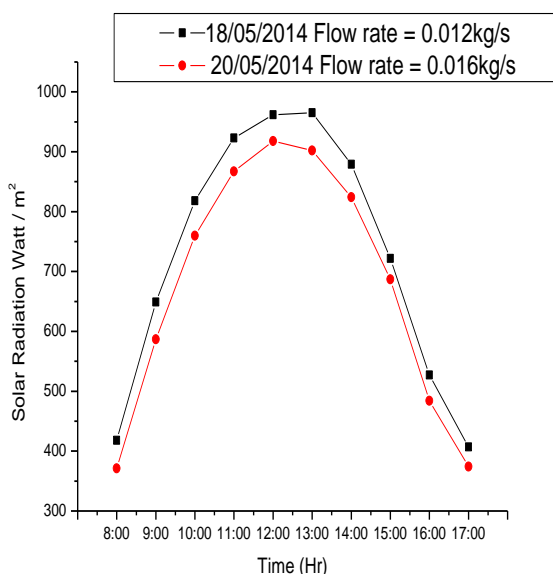


Figure 7 . Hourly variation of solar irradiation, for months of May.

Fig.7 shows the hourly variations of the measured solar radiation of different conditions of the days with flat plate absorber plate, corresponding months such as May. The highest daily solar radiation is obtained as 965 and 918 W/m^2 at solar air collector. It increases during the morning to some peak value and starts to decrease in the afternoon for all the days in which experiment was conducted as expected. Solar intensity is at their highest values at noon about 13: 00 as is expected. The solar intensity decreases as the time passes through the afternoon. The highest daily solar radiation is obtained as 965 and 918 W/m^2 at solar air collector. It increases during the morning to some peak value and starts to decrease in the afternoon for all the days in which experiment was conducted as expected.

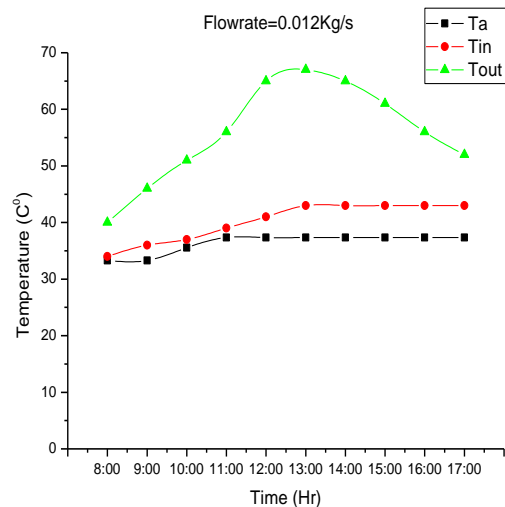


Figure 8. Temperature versus different standard local time during days for the flow rate at 0.012 Kg/s corresponding to the outlet, inlet, and ambient.

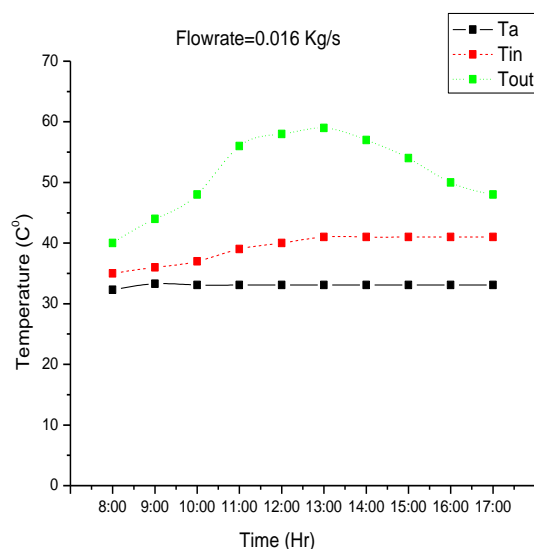


Figure 9. Temperature versus different standard local time during days for the flow rate at 0.016 Kg/s corresponding to the outlet, inlet, and ambient.

Fig. 8& 9 show the variation of the ambient, outlet and inlet temperatures as a function of air mass flow rates and time during day. The temperature was measured experimentally,

and it can be seen from graph that the curves of outlet temperature tend to decrease with increasing air mass flow rate. For a specific air mass flow rate at a constant ambient temperature, the outlet and inlet temperatures increase with increasing solar intensity. In general, the inlet temperature was found to be increasing exponentially from the morning for mass flow rates $m = 0.012 \text{ kg/s}$ and 0.016 kg/s . In particular; $T_{in} = 36^\circ\text{C}$ at 9:00h, for ambient temperature $T_a = 33.3^\circ\text{C}$. The thermal efficiency of the prototype geometrically constructed CPC solar collector is presented in Figure 10. The thermal output Q_u [inW] of collector was determined by measuring (with type-k thermocouples) the temperature rise of air flowing through the collector, and multiplying it by heat capacity C and mass flow rate m

$$Q_u = mc(T_o - T_i) \quad (27)$$

The flow rate was measured by digital anemometer. The most general equation used for the calculation of solar collector efficiency, which can be expressed as the ratio of the heat stored into collector to the total heat amount incident onto the collector during the same time,

$$\eta = \frac{mc(T_o - T_i)}{H_i A_a} \quad (28)$$

Where c = specific heat of air = 1009 J/kg-K

A_a = aperture area = $W \times L2$

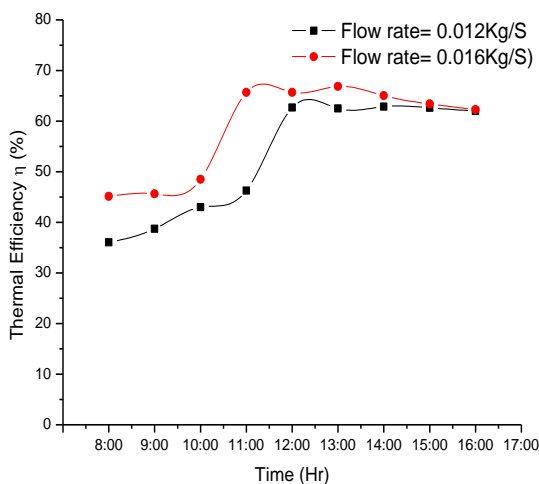


Figure 10. Collector efficiency with the local time

X. CONCLUSIONS

A number of runs with individual parameters varied while others held constant to find the influence of the air mass flow rate, collector length, and wind speed on the thermal performance of the present has been presented. A CPC with an aperture area of 1.2 m^2 , a real concentration ratio of 2, an acceptance half angle of 30° has designed and built. A numerical model was also carried out. Experiment tests were developed in a fluid operating range from 40°C to 90°C and with a mass flow rate from 0.012 and 0.016 kg s^{-1} to validate numerical model. Numerical model has proven to be reliable tool for the design and optimization of CPC for solar air dryer and validated with experimental data for the entire range of

operation conditions. The efficiency of the collector improves with increasing solar intensity at mass flow rate of 0.012 and 0.016 kg s^{-1} , due to enhanced heat transfer to the air flow. Optimum values of air mass flow rates are suggested to maximize the performance of the solar collector. The reason for the significant increase in efficiency from 0.012 and 0.016 kg s^{-1} can be attributed to changes in flow condition from laminar to turbulent. It could also be seen that slope of the efficiency curves decreases, meaning decrease in loss coefficient, with increase in mass flow rates. The air outlet temperature (66°C) attained by CPC is higher than available in FPC even when the CPC is flat. The stationary low cost CPC solar air heater with the concentration ratio of 2 suns has been proposed for air heating with specific advantages of no need of continuous tracking, no utmost accuracy required in fabrication, acceptance of diffuse radiation, saving of material by truncation, low loss and used for domestic up to small commercial size drying of crops, agricultural products and foodstuff, such as fruits, vegetables, aromatic herbs, wood, etc., contributing thus significantly to the economy of small agricultural communities and farms.

REFERENCES

- [1] Winston R. (1974) Principles of solar concentrators of a novel design. *SolarEnergy*16, 89-95.
- [2] Yan Q, Hu E, Yang Y, Zhai R. Dynamic modeling and simulation of a solar direct steam- generating system. *International Journal of Energy Research* 2010;34:1341–1355
- [3] Odeh S. D, Morrison GL. Optimization of parabolic trough solar collector system. *International Journal of Energy Research* 2006; 30:259 –271.
- [4] Kim Y, Han G, Seo T. An evaluation on thermal performance of CPC solar collector. *International Communications in Heat and Mass Transfer* 2008; 35:446 – 457.
- [5] Tchinda R, Ngos N. A theoretical evaluation of the thermal performance of CPC with flat one-sided absorber. *International Communications in Heat and Mass Transfer* 2006; 33:709–718.
- [6] Pramuang S, Exell THB. Transient test of a solar air heater with a compound parabolic concentrator. *Renewable Energy* 2005; 30:715–728.
- [7] Prapas DE, Norton B, Melidis PE, Probert SD. Convective heat transfers within air spaces of compound parabolic concentrating solar- energy collectors. *Applied Energy* 1998; 28:123–135.
- [8] Fraidenraich N, Lima R de CF, Tiba C, Barbosa EM de S. Simulation model of a CPC collector with temperature dependent heat loss coefficient. *Solar Energy* 1999; 65:99 –110.
- [9] Prasad B, Tiwari GN. Effect of glass cover inclination and parametric studies of concentrator-assisted solar distillation system. *International Journal of Energy Research* 1996; 20:495–505.
- [10] Winston, R., Minaco, J.C., Benitez, P., Shatz, N., & Bortz, J.C.(2005). *Nonimaging optics*, Elsevier Academic Press, London, UK.
- [11] D.K.Patel and P.K.Brahmbhatt (2014) 'Compound Parabolic Solar Concentrator with AutoLISP' Proc. 1st International Conference on MEET, Bhopal. pp 941-947.
- [12] Ellen Finkelstein (2006) *AutoCAD® and AutoCAD LT® Bible*, Wiley Publishing Inc. Indianapolis, Indiana.
- [13] Khonkar and Sayigh (1994) Raytrace for Compound parabolic concentrator, *Renewable Energy*, Vol-5, Part I, Pages 376-383.
- [14] Khonkar and Sayigh (1995) Optimization of the Tubular absorber using a Compound parabolic concentrator, *Renewable Energy*, Vol-6, No-1, Pages 17-21.

- [15] Rene T chinda .Thermal behavior of solar air heater with compound parabolic concentrator. *Energy conversion and Management* 49(2008) 529-540. Science Direct, Elsevier.
- [16] Duffie JA, Beckman WA. *Solar engineering of thermal process* New York: John Wiley and Sons; 1980.
- [17] D.K.Patel and P.K.Brahmbhatt (2014)'Computer Aided Design and Manufacture Of Compound Parabolic Solar Air Collector'' Proc. International Conference on Recent Trends in Engineering and Technology, Published by Elsevier, pp, 134-136
- [18] R.S.Gill,Sukhmeet Singh, Parm Pal Singh(2012) Low cost solar air heater , *Energy conversion and Management* 57(2012) 131-142. Science Direct, Elsevier.
- [19] Pei Gang,Li Jing, Ji Jie (2010) Analysis of low temperature solar thermal electric generation using regenerative Organic rankine Cycle. *Applied Thermal Engineering* 30 (2010) 998-1004. Dan Nchelatebe Nkwetta, Mervyns.
- [20] Smyth (2012) performance analysis and comparison of concentrated evacuated tube heat pipe solar collectors, *Applied Energy* 98 (2012) 22-32.

About Authors:



First Author D.K.Patel is presently working as Head of Department (Mechanical Engineering) at Government Engineering college, Patan-Gujarat. He is also a research scholar at Rai University, Ahmedabad. He has published 3 papers in international conferences. He has 3 years of experience in industry and 16 years of experience in teaching.



Second Author Dr. P.K.Brahmbhatt is presently working as Head of Department (Mechanical Engineering) at Government Engineering college, Modasa-Gujarat. He is also a research guide at Rai University, Ahmedabad. He has published more than 20 papers in international conferences and journals. He has 1 years of experience in industry and 16 years of experience in teaching.